The Canadian Mineralogist
Vol. 35, pp. 713-722 (1997)

RELATIVELY UNOXIDIZED VIVIANITE IN LIMNIC COAL FROM CAPENI, BARAOLT BASIN, ROMANIA

STEFAN MARINCEA[1]

Department of Mineralogy, Geological Institute of Romania, 1 Caransebes Street, RO-78344, Bucharest, Romania

EMIL CONSTANTINESCU

Department of Mineralogy, University of Bucharest, 1 Balcescu Bd., Romania

JEAN LADRIERE

INAN Laboratory, Catholic University of Louvain, Louvain-la-Neuve, B-1348, Belgium

ABSTRACT

Vivianite in limnic coal from Capeni, Baraolt Basin, Romania, is partially oxidized, despite the strongly reducing environment. The main reflections of its X-ray powder pattern may be indexed on a monoclinic cell with *a* 10.037(10), *b* 13.464(9), *c* 4.723(5) Å and β 102.55(4)° (space group *I2/m*) or *a* 10.113(14), *b* 13.464(9), *c* 4.723(5) Å and β 104.38(3)° (space group *C2/m*). The thermal analyses, taken in air, show effects attributable to the oxidation of Fe^{2+} to Fe^{3+} ions, *i.e.*, the splitting of the first endothermic effect at about 190°C, the presence of a supplementary exothermic peak at 270°C on the DTA curve, and a gradual dehydration on the TGA curve. The Mössbauer spectrum consists, however, of four quadrupole doublets associated with two sites occupied by ferrous iron and two occupied by ferric iron. Approximately 13% of Fe(2) and 15% of Fe(1) are oxidized to Fe^{3+}. The infrared absorption spectrum shows a splitting of the fundamental H–O–H stretching at 3000–3500 cm^{-1}, as well as the absence of an (OH) band at about 3370 cm^{-1}, confirming a slight oxidation of the sample analyzed. Chemical analyses show that only 18 to 22% of the iron is oxidized to Fe^{3+} and that less than 7.2% of the octahedra are occupied by cations other than iron. On the basis of the geological setting and trace-element chemistry, diagenetic formation in anoxic low-sulfide sediments is indicated. Partial oxidation is due to exposure to air following collection.

Keywords: vivianite, limnic coal, X-ray data, thermal behavior, Mössbauer spectroscopy, infrared-absorption data, crystal chemistry, oxidation, Capeni, Romania.

SOMMAIRE

La vivianite des charbons limniques de Capeni, du Bassin de Baraolt, en Roumanie, est partiellement oxydé, malgré le milieu encaissant fortement réducteur. Les réflexions principales de son spectre de diffraction X peuvent être indexées sur une maille monoclinique du groupe spatial *I2/m* avec *a* 10.037(10), *b* 13.464(9), *c* 4.723(5) Å et β 102.55(4)° ou du groupe spatial *C2/m* avec *a* 10.113(14), *b* 13.464(9), *c* 4.723(5) Å et β 104.38(3)°. Les analyses thermiques obtenues dans l'air montrent des effets causés par l'oxydation du Fe^{2+} à Fe^{3+}, comme le dédoublement du premier effet endothermique à environ 190°C, un effet exothermique supplémentaire à 270°C sur la courbe ATD et une déshydratation progressive sur la courbe TG. Le spectre de Mössbauer montre quatre doublets quadripolaires, associés aux deux sites à fer ferreux et aux deux à fer ferrique. Environ 13% du Fe(2) et environ 15% du Fe(1) sont oxydés à Fe^{3+}. Le spectre d'absorption infrarouge confirme le faible degré d'oxydation de l'échantillon analysé, confirmé par le dédoublement de la bande de vibration de valence H–O–H fondamentale à 3000–3500 cm^{-1}, et aussi par l'absence de la bande de l'hydroxyle à environ 3370 cm^{-1}. Les analyses chimiques confirment que seulement de 18 à 22% du fer est oxydé, et montrent que moins de 7.2% des positions octaédriques est occupé par des cations autres que le fer. Le contexte géologique et la géochimie des éléments en trace étayent l'hypothèse d'une formation diagénétique du minéral, dans un milieu anoxyque, pauvre en soufre. L'oxydation partielle des échantillons analysés est par conséquent due à leur exposition à l'air après le prélèvement.

Mots-clés: vivianite, charbon limnique, données de diffraction X, analyse thermique, spectroscopie de Mössbauer, spectrométrie d'absorption infrarouge, chimie cristalline, oxydation, Capeni, Roumanie.

---

[1] *E-mail address*: stefan@spin.emse.fr
Present address: École des Mines de Saint-Étienne, 158, Cours Fauriel, Saint-Étienne Cedex 2, France

INTRODUCTION

Vivianite is quite widespread in sedimentary fields in Romania. It is mentioned in pelitic and psammitic rocks by Cadere (1928) and Radulescu & Dimitrescu (1966), but has not been reported in coal. Nevertheless, occurrences in coal are mentioned by Palache *et al.* (1951) in Germany (Meklenburg) and France (Commentry, Cransac). In this paper, we describe a first occurrence of vivianite in Romanian coal. An extensive analytical investigation was deemed necessary in view of peculiarities due to the strongly reducing environment in coal deposits.

GEOLOGICAL SETTING

At Capeni (Baraolt Basin, Bârsei Depression, East Carpathians), vivianite has been found in lignite hosted by a sedimentary sequence of Pliocene age. Lignite in this deposit is a soft dull coal containing 30 to 50% by weight humodetrinite (Borcos *et al.* 1984). It occurs as beds included in a marly-sandy horizon that belongs to the post-tectonic cover of the Bârsei Depression. This horizon consists in an alternation of marl, tuffaceous marl and sand, with lignite intercalations. The palynological content indicates a Pliocene age, whereas the microfauna and the sedimentary environment suggest a limnic origin for the whole sequence.

An X-ray-diffraction study of the mineral content of the Capeni coal led to the identification, in addition to vivianite, of kaolinite, illite, gypsum, pyrite, marcasite, quartz, K-feldspar and calcite. Furthermore, some minor minerals, such as interlayered illite-smectite, siderite and iron sulfates with various degrees of hydration (*i.e.*, szomolnokite, melanterite, jarosite) also occur.

Vivianite forms earthy nodular aggregates enclosed by marl that contains abundant coaly organic matter. These marly sequences invariably occur near the limit between the coal beds and the surrounding pelites, and are commonly interbedded with pure coal. The nodules of vivianite range from a few mm to more than 4 cm in diameter. They have a round shape, a spheroidal to discoidal development, and a rough surface. The constituent crystals, up to 0.1 mm in size, are very closely packed and randomly oriented.

PHYSICAL PROPERTIES

A microscopic study shows that the blue-indigo color of the earthy concretions, which indicates a certain degree of oxidation, has a strong pseudochromatic nature. The flat, prismatic crystals studied in immersion are translucent to transparent and are pleochroic in light blue (α) to light green shades (β and γ). Polysynthetic twins on (010), usually recorded in oxidized vivianite (Dormann *et al.* 1982), were not observed.

The mean indices of refraction, determined in immersion using oblique illumination and sodium light (λ = 589 nm) vary between 1.63(1) and 1.65(2). The average indices of refraction, calculated from the composition in Table 1 (sample 2) and measured densities, according to the Gladstone–Dale law (Mandarino 1976), are n = 1.649(5) and n = 1.652(2), respectively, in reasonable agreement with the measured values.

A change in the macroscopic color, from indigo blue to brown, occurs after heating at 100°C, and indicates a rapid superficial oxidation followed by a partial dehydration.

The density of a vivianite aggregate, measured at 22°C by means of a pyknometer, using toluene as displacement fluid, is 2.70(1) g/cm^3. It agrees well with the value of 2.69(2) g/cm^3 established for isolated crystals by sink–float in bromoform–toluene solutions. Both values are slightly lower than that calculated on the basis of the molecular weight deduced from the chemical data in Table 1 (sample 2) and using the cell parameters in Table 2, *i.e.*, 2.718 g/cm^3. The differences are, however, minor, and may be due to the different degrees of oxidation of the samples analyzed.

TABLE 1. CHEMICAL COMPOSITION OF VIVIANITE FROM CAPENI

OXIDE	SAMPLE 1*	SAMPLE 2*	SAMPLE 3**	SAMPLE 4**	SAMPLE 5**
Fe_2O_3	8.50	10.27	9.307 (3)	9.401 (3)	9.158 (3)
FeO	34.47	32.34	33.169	33.505	32.643
MnO	-	0.92	0.922	1.284	0.923
CaO	-	0.14	0.379	0.216	0.267
MgO	-	0.60	0.505	0.938	0.756
P_2O_5	28.22	26.91	27.966	29.393	27.831
H_2O	28.70	28.38	27.752 (2)	25.263 (2)	28.422 (2)
Total	99.89	99.56 (1)	100.00	100.00	100.00
NUMBER OF IONS ON THE BASIS OF 2 P ATOMS					
Fe^{3+}	0.536	0.678	0.592	0.568	0.585
Fe^{2+}	2.413	2.381	2.344	2.252	2.317
Mn	-	0.069	0.066	0.087	0.066
Ca	-	0.013	0.034	0.018	0.025
Mg	-	0.078	0.064	0.112	0.096
P	2.000	2.000	2.000	2.000	2.000
$(OH)^-$	0.434	1.116	0.792	0.642	0.763
H_2O	7.566	6.884	7.208	7.358	7.237

* wet-chemical analyses. Results reported in weight %.

** microprobe analyses. Mean of 4, 5, 5 point analyses.

(1) includes 14.73 % H_2O^+ and 13.65 % H_2O^-.

(2) deduced by difference.

(3) assumed on the basis of wet-chemical tests.

TABLE 2. CELL PARAMETERS OF SELECTED SAMPLES OF VIVIANITE

a. REFINED IN SPACE GROUP C 2/m

LOCATION	REFERENCE	a (Å)	b (Å)	c (Å)	β
(?)	Yamaguti (1936)*	9.997	13.370	4.696	104.27°
Monserrat (Bolivia)	Barth (1937)	10.039	13.388	4.687	104.30°
Ashio (Japan)	Mori & Ito (1950)	10.08	13.43	4.70	104.50°
Huanuni (Bolivia)	Fejdi *et al.* (1980)	10.086	13.441	4.703	104.27°
Kamysh-Burun (Russia)	Dormann *et al.* (1982)	10.117	13.394	4.684	104.70°
Capeni (Romania)	this work	10.113	13.464	4.723	104.38°

b. REFINED IN SPACE GROUP I 2/m

LOCATION	REFERENCE	a (Å)	b (Å)	c (Å)	β
(?)	Yamaguti (1936)**	9.962	13.40	4.70	102.62°
Monserrat (Bolivia)	Barth (1937)**	9.975	13.388	4.687	102.78°
Ashio (Japan)	Mori & Ito (1950)**	9.99	13.43	4.70	102.57°
Lake Biwa (Japan)	Nakano (1992)	10.05	13.51	4.70	102.41°
- (SYNTHETIC)	PDF 30-0662	10.034	13.449	4.707	102.65°
Capeni (Romania)	this work	10.037	13.464	4.723	102.55°

* as given by Barth (1937).

* * as calculated by Donnay *et al.* (1963).

THERMAL ANALYSES

The thermal curves for a sample of vivianite from Capeni are given in Figure 1. They were drawn using a MOM 1500 D derivatograph used with a Pt–Pt Rh thermocouple, at a mean rate of heating of 10°C per min., in air. The vivianite used for analysis, as well as for other measurements, was gently pulverized by mechanical grinding under acetone, then dried in flowing nitrogen, in order to reduce oxidation.

The thermal behavior of vivianite, and particularly its differential thermal responses, has been studied extensively. As mentioned by Rodgers & Henderson (1986) and Rodgers (1989), all previous studies showed that the major differential thermal effects between 20°C and 1000°C are basically attributable to a series of dehydrations and structural reorganization. Our interpretation of the thermal curves in Figure 1 confirms this inference.

The doublet of endothermic peaks recorded on the differential thermal analysis (DTA) curve at 183°C and 205°C, respectively (178° and 200°C on the differential thermogravimetric, DTG curve), marks a major loss of structurally bound H_2O. The splitting of this major endotherm is obviously due to an overlapped exothermic effect, which clearly marks the beginning of oxidation of Fe^{2+} to Fe^{3+} (Dormann *et al.* 1982). The weight loss calculated for this step on the basis of the thermogravimetric (TGA) curve is of about 15.5 wt.%, similar to the loss reported by Dormann *et al.* (1982) for a slightly oxidized sample of vivianite from Anloua (Cameroon). The total loss in weight recorded by this curve, 24% in conditions of a weak increase in weight induced by the oxidation [+4.7% according to Dormann *et al.* (1982)], suggests that the calculated loss of H_2O approximates 5.2 molecules. This agrees with earlier determinations of Manly (1950) and Kleber *et al.* (1965), who estimated that this first endotherm corresponds to the depletion of five molecules of structurally bound H_2O.

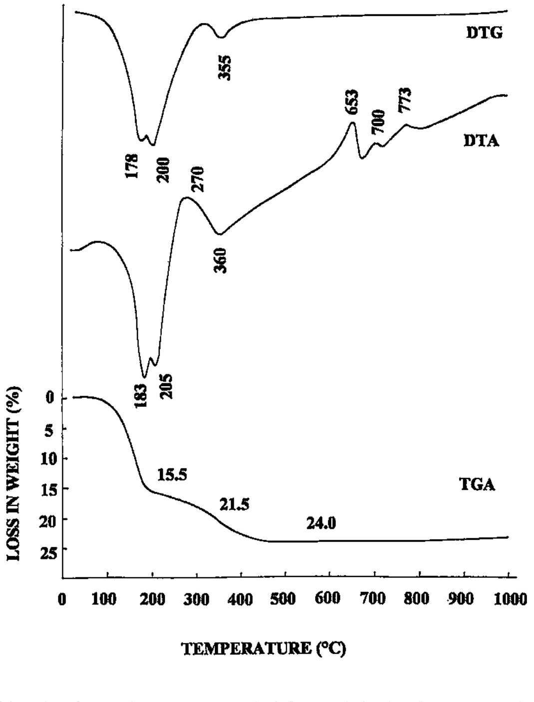

FIG. 1. Thermal curves recorded for a vivianite from Capeni: differential thermogravimetric (top), differential thermal analysis (middle) and thermogravimetric (bottom).

The exothermic peak recorded on the DTA curve at 270°C corresponds to another phase of oxidation of Fe^{2+} to Fe^{3+}. Such an effect was not reported by Tien & Waugh (1969) or by Dormann *et al.* (1982), but was found by Rao (1965) at 250°C and by Vochten *et al.* (1979) at 260°C, and assigned to a phase transformation (Vochten *et al.* 1979).

The endothermic effect marked at 360°C on the DTA curve (355°C on the DTG curve) is essentially related to the loss of another two molecules of H_2O, though that loss in H_2O may be rather regarded as a dehydroxylation of a transitional phase than as a true dehydration (Dormann *et al.* 1982). The cumulative loss in weight recorded on the TGA curve is about 21.5 wt.%, which represents about 90% of the total H_2O lost.

An important feature of the thermal record (Fig. 1) is the absence of another endothermic effect, found by Manly (1950), Rao (1965), Kleber *et al.* (1965) and Tien *et al.* (1969) on the DTA curves of many samples, between 380 and 470°C. A similar behavior was, however, reported by Bocchi *et al.* (1971) for vivianite from Anloua (Cameroon) and can be easily regarded as a progressive loss of the last molecule of H_2O, bound as hydroxyl groups in some ferric hydroxy-metaphosphates. The end of the decrease in weight marked on the TGA curve corresponds to a temperature of about 470°C, the same as that reported by Tien *et al.* (1969) for the end of the dehydration of vivianite from Kansas. The total weight-loss recorded on the TGA curve is 24 wt.%. After the theoretical correction of (+) 4.7 wt.% due to the oxidation of Fe^{2+} to Fe^{3+}, this loss closely approximates the total H_2O content determined by using the Penfield method (28.38 wt.%).

The exothermic effect recorded at 653°C on the DTA curve marks a major structural transformation that brings about the formation of α-$FePO_4$, $Fe(PO_3)_3$ and, occasionally, γ-Fe_2O_3 (maghemite) (Rodgers & Henderson 1986, Rodgers 1989). Subsequently, a gradual structural reorganization, a polymorphic transformation according to Tien & Waugh (1969) gives two other small exotherms at 700 and 773°C, respectively (Fig. 1).

The fusion (or decomposition), which usually occurs between 1000 and 1200°C (Rodgers & Henderson 1986), is announced by the beginning, on the DTA and DTG curves, of an endothermic effect in the range

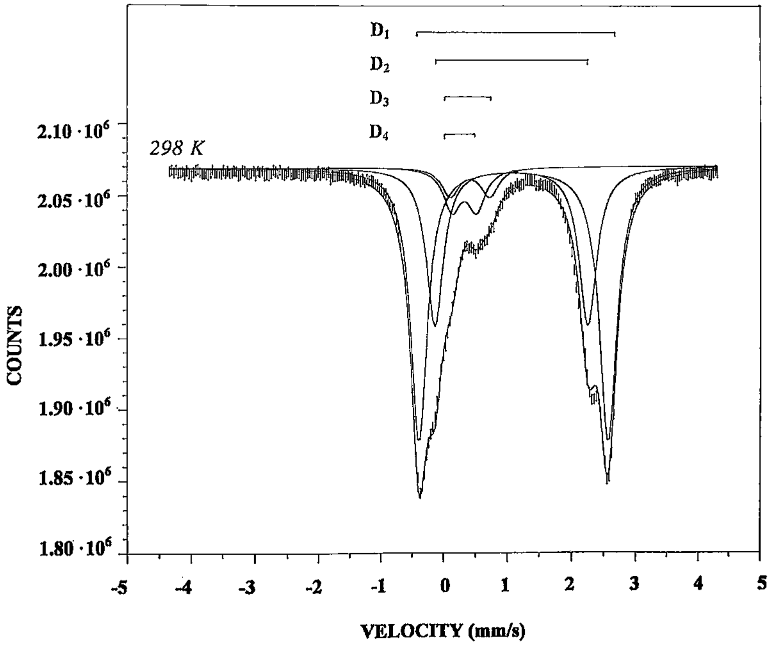

FIG. 2. Room-temperature ^{57}Fe Mössbauer spectrum of vivianite from Capeni. Quadrupole doublets are indicated on top.

980°C and 970°C, respectively. This effect is visible with difficulty in Figure 1 because of drift in the apparatus, but it was clearly recorded at a lower heating rate, 5°C/min.

An X-ray powder-diffraction study of the breakdown products obtained after heating at 1000°C and cooling in air indicates the presence, as a major phase, of the ferric orthophosphate (α-$FePO_4$: PDF 29–0715). The main reflections recorded for this compound [*d* in Å(*I*)] occur at 3.461(100), 4.382(25), 2.362(15), 2.180(15), 1.871 (15) and 1.623(10). Some supplementary reflections are attributable to admixed hydrous ortho- and metaphosphates.

Although the differences in thermal behavior between unoxidized and oxidized vivianite or between vivianite and metavivianite are too slight to be used for discrimination (Rodgers & Henderson 1986), vivianite from Capeni behaves as a typical unoxidized or moderately oxidized vivianite. This conclusion is supported by the recording in its thermal curves of all the effects that are generally attributable to the $Fe^{2+} \rightarrow Fe^{3+}$ transition in such compounds, *i.e.*, the splitting of the first endotherm, a supplementary exothermic peak at 270°C on the DTA curve, and a gradual dehydration on the TGA curve.

MÖSSBAUER SPECTROSCOPY

Mössbauer spectroscopy has been used by many authors to estimate the degree of natural or artificial oxidation of vivianite. Thus, the studies of Vochten *et al.* (1979), De Grave *et al.* (1980), McCammon & Burns (1980), Dormann & Poullen (1980), and Dormann *et al.* (1982) show that the Mössbauer spectra of oxidized vivianite can be described by means of four quadrupole doublets. They differ from the spectra of unoxidized vivianite, which show only two quadrupole doublets (Gonser & Grant 1967, Mattievich & Dannon 1977).

This different behavior has a structural explanation. Crystal-structure refinements reported by Mori & Ito (1950) and by Fejdi *et al.* (1980) show that, in vivianite, the octahedrally coordinated iron occupies two different structural sites, namely Fe(1) and Fe(2). Iron in the Fe(1) sites is found to be six-fold-coordinated to four H_2O ligands in a rhombic plane and by two *trans* oxygen atoms belonging to $(PO_4)^{3-}$ groups. The Fe(2) sites are coordinated by two H_2O ligands in *cis* position and by four atoms of oxygen belonging to $(PO_4)^{3-}$ groups. As a result, the Mössbauer spectra of unoxidized vivianite could be decomposed into two sets of asymmetric quadrupole-split doublets associated with the two ferrous-iron-bearing sites (Gonser & Grant 1967, Mattievich & Danon 1977). The number of quadrupole splits is obviously double in oxidized vivianite because analogous ferric-iron-bearing sites occur.

The ^{57}Fe Mössbauer spectroscopy was consequently considered appropriate for the study of the degree of oxidation of our mineral. A Mössbauer spectrum was

TABLE 3. MÖSSBAUER HYPERFINE PARAMETERS, RELATIVE IRON DISTRIBUTIONS (α) AND SITES ASSIGNMENT FITTED TO THE SPECTRUM IN FIGURE 2 *

SAMPLE	QUADRUPOLE DOUBLET	I.S. (mm/s)	Q.S. (mm/s)	α (%)	SITE	Fe^{2+}/ Fe^{3+}	Fe(2)/ Fe(1)
VIVIANITE	D_1	1.17(3)	2.38(5)	31.6	$Fe^{2+}(1)$		
FROM	D_2	1.20(3)	2.95(5)	54.6	$Fe^{2+}(2)$		
CAPENI	D_3	0.53(3)	0.61(5)	5.7	$Fe^{3+}(1)$	6.25	1.68
	D_4	0.44(3)	0.38(5)	8.1	$Fe^{3+}(2)$		
SYNTHETIC	D_1	1.15(3)	2.51(5)	33.3	$Fe^{2+}(1)$		
VIVIANITE	D_2	1.20(3)	2.97(5)	66.7	$Fe^{2+}(2)$	∞	2.00

* as compared with similar data given by Mattievich & Danon (1977) for synthetic vivianite.

obtained on a time-mode spectrometer, using a constant-acceleration drive. A ^{57}Co source was used in a Rh matrix, with an initial activity of 5 mCi. The spectrum was recorded at 298 K. The hyperfine parameters were determined by fitting a sum of Lorentzian lines to the experimental Mössbauer spectrum, using a least-squares iterative program.

The spectrum (Fig. 2) can be described satisfactorily by four quadrupole doublets, referred as D1, D2, D3 and D4 by Vochten *et al.* (1979); these mark the two ferrous-iron and two ferric-iron sites. The spectrum shows excellent agreement with the ones given by Vochten *et al.* (1979), Dormann & Poullen (1980), Dormann *et al.* (1982) and Nembrini *et al.* (1983) for partially oxidized vivianite. The hyperfine parameters, isomer shift I.S. (δ) and quadrupole splitting Q.S. (Δ) obtained, the relative distributions of iron in ferrous-iron and ferric-iron sites (α), and the assignment of the four doublets to the various iron species, are presented in Table 3. The assignment of the Fe^{2+} doublets is based on the values of the isomer shift and of the quadrupole splitting found in pure vivianite by Mattievich & Danon (1977); these also are given in Table 3. The two Fe^{3+} doublets were ascribed to the (1) and (2) sites in order to maintain a Fe(2):Fe(1) ratio that approximates 2:1, as expected. Taking into account the results, we estimate that 13% of Fe(2) and about 15% of Fe(1) are Fe^{3+}. This finding agrees very well with the structural premises (iron coordinated to four H_2O ligands is more easily oxidizable) and with chemical data given below.

INFRARED ABSORPTION STUDY

An infrared absorption spectrum of a vivianite sample from Capeni was recorded in the frequency range between 250 and 4000 cm^{-1} using a SPECORD M–80 spectrometer. The spectrum was obtained using the standard pressed-disk technique, after embedding a small amount of mechanically ground vivianite (2.5 wt.%) in dry KBr and compacting under 2500 N/cm^2 pressure. The spectrum is given in Figure 3, together with a similar spectrum recorded for a sample of slightly oxidized vivianite from Anloua (Cameroon).

The main absorption bands are attributable to the vibrational modes of the hydrogen-bonded systems (hydroxyl groups, water of crystallization and adsorbed water) and of the $(PO_4)^{3-}$ groups. Their assignment is substantially facilitated by the previous results of Brunel & Vierne (1970), Vochten *et al.* (1979) and Piriou & Poullen (1987). The assignment of the main bands recorded in the two samples analyzed is consequently attempted in Table 4.

An estimation of the degree of oxidation has been attempted on the basis of the infrared absorption data. The relevant structural effect of the substitution of the H_2O ligands by hydroxyl groups, which follow the Fe^{2+} to Fe^{3+} transition, is considered to be the distortion of the octahedra of the structure (Piriou & Poullen 1987). The resultant effect on the infrared spectrum is the decrease in the intensity of the absorption bands around 3450 and 3160 cm^{-1} (Piriou & Poullen 1987). These bands, which express the ν_3 antisymmetric stretching of the H_2O molecules, are very strong in the infrared spectrum of our material (Fig. 3). This fact, as well as the evident splitting of the 3000–3500 cm^{-1} band, indicates the presence at Capeni of vivianite *sensu stricto*. On the other hand, the lack of the band at about 3260 cm^{-1}, which expresses the ν_1' symmetric stretching of H_2O in unoxidized vivianite (Piriou & Poullen 1987), indicates a certain degree of oxidation. In both analyzed samples, this 3260 cm^{-1} absorption band is absent and not covered by another one at about 3370 cm^{-1}, found in metavivianite and assigned to $(OH)^-$ groups (Piriou & Poullen 1987). This behavior is quite normal since the 3370 cm^{-1} band is weak or absent in the spectra of vivianite *sensu stricto*. We conclude that the vivianite from Capeni is only slightly oxidized and does not contain any admixed metavivianite.

As can be seen in Table 4, the main absorption bands due to the $(PO_4)^{3-}$ groups lie in the 900 to 1000 cm^{-1} and 500 to 600 cm^{-1} regions. Both stretchings in the first spectral range and bendings in the second were practically recorded at the same frequencies by Tien & Waugh (1969), Brunel & Vierne (1970) and Vochten *et al.* (1979). It seems, therefore, that the position of the absorption bands due to this functional molecular group is not dependent on interatomic environment (*e.g.*, on Fe^{2+} to Fe^{3+} transitions).

More relevant in this respect seem to be the low-frequency bands between 250 and 600 cm^{-1}, and particularly those below 400 cm^{-1}, which in the majority of cases can be assigned to the internal vibrations of octahedra, and which express metal–oxygen stretching and bending modes (Brunel & Vierne 1970, Vochten *et al.* 1979). As the different extents of the iron oxidation in the samples induce differences in the bond strengths, the vibrational frequencies are expected to vary as a function of degree of oxidation. A comparison of our

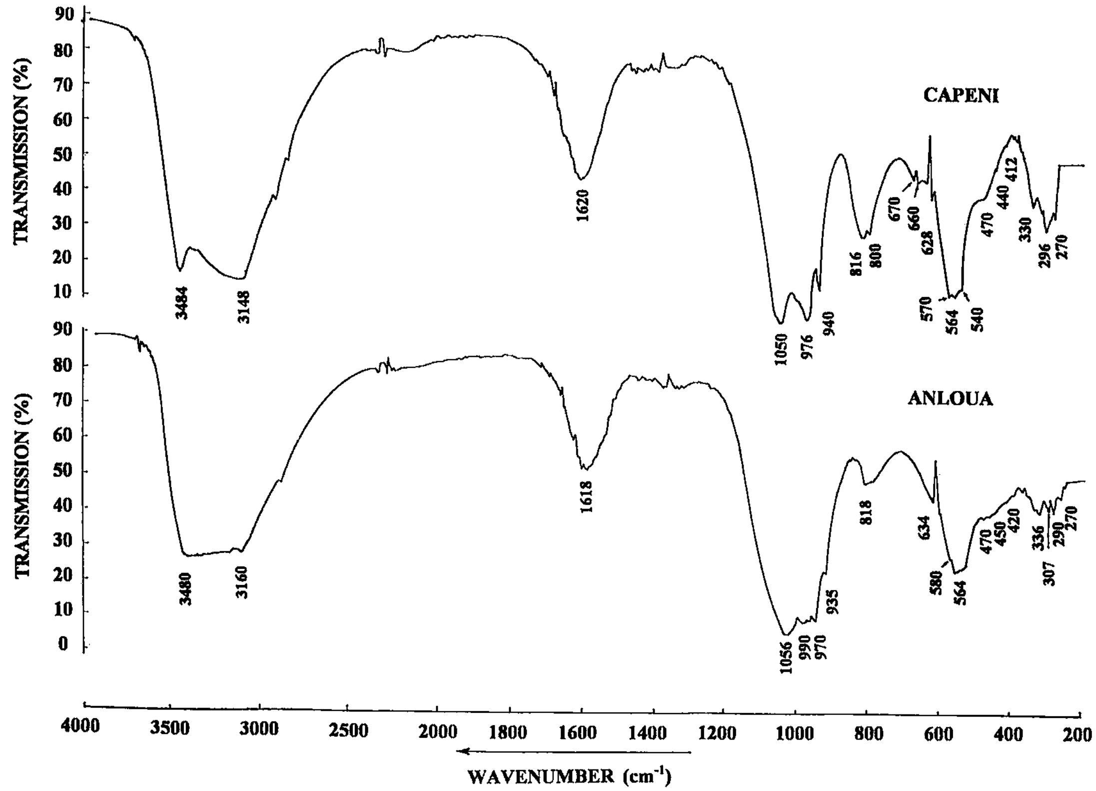

FIG. 3. Infrared spectra of vivianites from Capeni (top) and Anloua (bottom).

data with those of Vochten *et al.* (1979) for unoxidized vivianite from Anloua, Cameroon (which absorbs at 268 cm^{-1}, 304 cm^{-1}, 368 cm^{-1}, *etc.*) and for oxidized vivianite from Retie, Belgium (which absorbs at 272 cm^{-1}, 292 cm^{-1}, 330 cm^{-1}, *etc.*) indicates that the Capeni vivianite is only slightly oxidized.

TABLE 4. POSITIONS AND ASSUMPTIONS CONCERNING THE INFRARED ABSORPTION BANDS RECORDED FOR VIVIANITE FROM CAPENI AND ANLOUA

Structural group	Vibrational mode	Capeni	Anloua
H_2O	ν_3' antisymmetric stretching	3484 cm^{-1}	3480 cm^{-1}
H_2O	ν_3 antisymmetric stretching	3148 cm^{-1}	3160 cm^{-1}
H_2O	H-OH bending	1620 cm^{-1}	1618 cm^{-1}
$(PO_4)^{3-}$	ν_3 antisymmetric stretching	1050 cm^{-1}	1056 cm^{-1}
$(PO_4)^{3-}$	ν_1' symmetric stretching	976 cm^{-1}	970 cm^{-1}
$(PO_4)^{3-}$	ν_1 symmetric stretching	940 cm^{-1}	935 cm^{-1}
H_2O	π (1)	816 cm^{-1}	818 cm^{-1}
H_2O	π (1)	800 cm^{-1}	-
-	metal-oxygen vibration (2)	670 cm^{-1}	-
-	metal-oxygen vibration (2)	660 cm^{-1}	-
H_2O (?)	(OH) libration (?)	628 cm^{-1}	634 cm^{-1}
-	metal-oxygen vibration (2)	570 cm^{-1}	580 cm^{-1}
$(PO_4)^{3-}$	ν_4' antisymmetric bending	564 cm^{-1}	564 cm^{-1}
-	metal-oxygen vibration (2)	540 cm^{-1}	-
$(PO_4)^{3-}$	ν_4 antisymmetric bending (3)	470 cm^{-1}	470 cm^{-1}
-	metal-oxygen vibration (3)	440 cm^{-1}	450 cm^{-1}
$(PO_4)^{3-}$	ν_2 symmetric bending (3)	412 cm^{-1}	420 cm^{-1}
-	metal-oxygen vibration (3)	330 cm^{-1}	336 cm^{-1}
-	metal-oxygen vibration (3)	296 cm^{-1}	290 cm^{-1}
-	metal-oxygen vibration (3)	270 cm^{-1}	270 cm^{-1}

(1) assigned by Brunel & Vierne (1970) to the H_2O ligands in the $FeO_4(H_2O)_2$ and $FeO_2(H_2O)_4$ groups.
(2) assumed by Brunel & Vierne (1970).
(3) as supposed by us.

X-RAY POWDER-DIFFRACTION DATA

The X-ray powder-diffraction analysis of a vivianite sample from Capeni was performed with an automated Siemens D–5000 Krystalloflex diffractometer, using graphite-monochromatized Cu*K*α radiation (λ = 1.54056 Å), at 40 kV and 30 mA. The pattern was collected in a 2θ range 10–45°, using a step size of 0.04° 2θ and a 2-second counting time at each step. Synthetic silicon, with an *a* of 5.4309 Å (PDF 27–1402) was used as internal standard. The data obtained are given in Table 5, together with those given by Sameshima *et al.* (1985) and in PDF 30–662 for synthetic $Fe_3(PO_4)_2{\cdot}8H_2O$.

The pattern shows that the vivianite from Capeni does not contain admixed metavivianite. No reflections are assignable to this mineral, and particularly the prominent ones close to 8.6 and 2.8 Å respectively,

TABLE 5. X-RAY POWDER-DIFFRACTION DATA FOR VIVIANITE FROM CAPENI* AND FOR SYNTHETIC $Fe_3(PO_4)_2 \cdot 8H_2O$

Crt. no.	CAPENI d_{obs}(Å)	d_{calc}(Å)	I / I_0	SYNTHETIC d_{obs}(Å)$^{(1)}$	d_{obs}(Å)$^{(2)}$	I / I_0	(hkl)
1	7.9712	7.9218	14	7.89	7.93	13	(110)
2	6.7481	6.7322	100	6.71	6.73	100	(020)
3	4.9014	4.8984	20	4.90	4.90	12	(200)
4	4.3587	4.3615	3	4.40	4.341	2	(011)
5	4.0689	4.0804	10	4.10	4.081	12	(130)
6	3.8509	3.8605	11	3.88	3.849	7	(101)
7	3.6484	3.6516	3	3.65	-	-	(-211)
8	3.2198	3.2158	17	3.22	3.210	16	(031)
9	2.9876	2.9887	20	2.99	2.985	10	(-301)
10	2.9760	2.9683	21	-	2.960	8	(211)
11	2.7140	2.7316	15	2.73	2.728	9	(-321)
12	2.7140	2.7106	15	-	2.706	9	(-141)
13	2.6379	2.6406	7	2.65	2.637	6	(330)
14	2.5989	2.5966	3	-	2.593	4	(-150)
15	2.5328	2.5371	10	2.54	2.530	8	(141)
16	2.4267	2.4275	10	2.44	2.421	6	(301)
17	2.3216	2.3253	5	2.33	2.321	7	(051)
18	2.2360	2.2349	8	2.25	2.233	5	(-341)
19	2.1820	2.1807	7	2.20	2.173	2	(022)

* Cu K_α, $\lambda = 1.54056$ Å.
(1) data from Sameshima *et al.* (1985).
(2) data from PDF 30-0662.

mentioned by Sameshima *et al.* (1985). Some additional reflections were found, however, at 7.019, 3.998, 3.485 and 2.821 Å. Except for the first and the third, these are barely visible above background. These reflections are coincident with or close to the lines of bobierrite at 6.96, 4.00, 3.48 and 2.81 Å, mentioned by Frazier *et al.* (1963). Taking into account the possibility that some other lines of bobierrite are obscured by vivianite reflections, and the detection of a bobierrite-like phase by Sameshima *et al.* (1985) in many vivianite admixtures, it appears that bobierrite also is present at Capeni.

A monoclinic cell of vivianite, with *a* 10.037(10), *b* 13.464(9), *c* 4.723(5) Å, β 102.55(4)° (space group *I2/m*) was found to correctly describe the average diffraction-symmetry of all the reflections given in Table 5. The cell parameters were determined by five cycles of least-squares refinement of the data in the table, using the computer program of Appleman & Evans (1973), as revised for microcomputer use by Benoit (1987). All the reflections in Table 5 could be also indexed in space group *C2/m*, found for vivianite by Mori & Ito (1950) and by Fejdi *et al.* (1980). A monoclinic cell with *a* 10.113(14), *b* 13.464(9), *c* 4.723(5) Å, β = 104.38(3)° could also be used to describe the structure.

In both cases, the cell parameters obtained are in good agreement with those quoted for a number of natural specimens (Table 2). The derived unit-cell volume *V*, 623.001 Å^3 is for $Z = 2$; considering as average composition that of sample 2 in Table 1 gives a calculated density of 2.718 g/cm^3. This value is in excellent agreement with values quoted by Donnay *et al.* (1963) for vivianite from some other occurrences ($2.70 < D_x < 2.72$ g/cm^3). Our value must reflect, therefore, a certain degree of oxidation of the sample, which normally induces a decrease in weight due to the replacement of (OH) for H_2O.

CHEMICAL DATA

Material for wet-chemical analysis was selected by hand-picking and magnetic separation. A partial and a complete analysis on two different separates (samples 1 and 2 in Table 1) were carried out in order to test the variability of the oxidation state of iron. The concentration of P was determined by gravimetry (Maxwell 1968), and that of Mn, Ca, and Mg, by atomic absorption spectrometry. The FeO content was determined titrimetrically following a modified Pratt method (Maxwell 1968), whereby Fe^{2+} is titrated in a boric–phosphoric hydrofluoric acid medium against $K_2Cr_2O_7$, using barium diphenylamine sulfonate as an indicator. The total iron content was determined by the volumetric method of Hume & Kolthoff (1957), from which the Fe_2O_3 content was obtained in a straightforward manner. As expected, a difference between the two samples occurs, but both analyses confirm the slight oxidation previously inferred: 18.2 and 22.2% of the iron, respectively, is oxidized to Fe^{3+}. This normally induces the substitution of some H_2O ligands by $(OH)^-$ groups and the occurrence of these groups into formulae. As a consequence, the formula approximates closely to $Fe^{2+}_{3-x}\,Fe^{3+}_{x}\,(PO_4)_2\,(OH)_x \cdot (8-x)\,H_2O$, where $x \leq 1.2$ (Gamidov & Mamedov 1960, Dormann & Poullen 1980). Their proposed formula does not consider the presence of some other octahedrally coordinated cations such as Mn^{2+}, Ca or Mg, and also supposes a stoichiometric proportion of P. Although the partial composition in Table 1 fits close to a 100% sum of wt.% oxides, showing that the isomorphous substitutions of Fe^{2+} by Mn^{2+}, Ca and Mg are minor, the other composition in the table indicates their presence.

Columns 3–5 represent results of electron-microprobe analyses on three separate grains, taken as an average of 4–5 random spot-analyses per grain. They were performed using a Cameca SX 50 microprobe. Operating conditions were 15 kV accelerating potential and 20 nA sample current on brass. Because the difficulties in performing electron-microprobe analyses on hydrated minerals such as vivianite (Autefage & Fontan 1985), the counting time was reduced at 10 s, and a slightly defocused beam was used. The standards used were fluorapatite (P, Ca), hematite (Fe), rhodonite (Mn) and synthetic forsterite (Mg). The oxidation state of iron was assumed on the basis of wet-chemical tests. Consequently, a Fe_2O_3:FeO ratio of 1:3.6, calculated as mean of the two wet-chemical determinations in Table 1, was applied to results of the microprobe analyses.

Taking into account the structural and compositional data reported before, the compositions in Table 1 were calculated on the basis of 4 P atoms (or 8 atoms of oxygen in the anhydrous and unhydroxylated compound). The general formula proposed by Gamidov & Mamedov (1960) was accepted as a basis for the calculations, and the proportions of $(OH)^-$ and H_2O were deduced following their scheme: $(OH)^-$ in order to maintain charge balance, and H_2O by difference. Mn was assumed to be in divalent state of oxidation.

The structural formulae show that: (1) The sum of Fe^{2+}, Mn^{2+}, Mg, Ca and Fe^{3+} invariably exceeds the stoichiometric number of 3 *apfu*. The slight excess over the stoichiometric proportion allowed in vivianite indicates the oxidation of Fe^{2+} to Fe^{3+} and shows that only relatively small amounts of $(OH)^-$ may proxy for $(PO_4)^{3-}$. (2) Manganese, generally recognized as the main isomorphous substituent of iron in vivianite (Palache *et al.* 1951, Ritz *et al.* 1974, Nakano 1992), is not abundant at Capeni: 2.1 to 2.9% of the iron positions are occupied by manganese. Even considering the presence of other substituents such as Ca or Mg, the analyzed sample of vivianite is remarkably pure: fewer than 7.2% of the octahedral positions are occupied by other cations than iron. (3) As expected, the number of hydroxyl groups per formula unit does not exceed the limit of 1.2, beyond which the monoclinic structure of vivianite collapses to the triclinic symmetry of metavivianite (Dormann & Poullen 1980, Dormann *et al.* 1982).

As can be seen in Table 1, differences between the results of a complete wet-chemical analysis and the mean of the electron-microprobe analyses 3–5 are minor. Consequently, the second composition listed in the table was considered as an average one and used for the calculation of the molecular weight. The accepted average composition corresponds to the higher degree of oxidation of the investigated samples. It leads to the formula: $(Fe^{2+}_{2.381}Mn^{2+}_{0.069}Ca_{0.013}Mg_{0.678})Fe^{3+}_{0.678}(PO_4)_2(OH)_{1.116}\cdot 6.884\ H_2O$, used for the calculation of molecular weight, 509.984 mass units, which gives the reported D_x.

Gladstone–Dale constants (Mandarino 1981) were used to calculate a compatibility index of 0.016, indicating superior agreement among the average optical, physical and chemical data.

A study of trace-element concentrations in the vivianite from Capeni confirms the purity of the sample. It was carried out by means of inductively coupled plasma – emission spectrometry, using a JOBIN–YVON 138 ULTRACE spectrometer. Only the siderophile elements such as Co (34.2 ppm), Ni (17.7 ppm), Zn (43.7 ppm) are well represented. They suggest, as well as the contents of Sc (5.5 ppm), Nb (3.4 ppm), Ti (10 ppm) and Th (2 ppm), some diadochic replacements of iron. An unusual enrichment in Ba (27.7 ppm) and the presence of Sr (2.4 ppm) are reported for a calcium content of 0.15%.

The rare-earth elements (*REE*) are deficient in the Capeni vivianite: the sample contains 8.94 ppm Y, 3.77 ppm La and 3.40 ppm Yb, which indicates a strong deficiency with respect to "normal" concentrations in sedimentary materials, approximately 230 ppm according to Herrmann (1978). The chondrite-normalized concentrations of the *REE*, with chondrite values from Herrmann (1978), illustrate a slight fractionation, since $(La/Yb)_N = 0.49$. Note that the heavy *REE* predominate over the light ones, as expected in lacustrine deposits.

DISCUSSION

Generally, vivianite forms either from hydrothermal solutions or by direct precipitation from groundwater. It is obvious that at Capeni, hydrothermal activity need not be considered. A sedimentary-diagenetic mode of formation seems likely.

Rosenqvist (1970), Nembrini *et al.* (1983), Manning *et al.* (1991) and Nakano (1992), among others, speculated that aggregates of vivianite can grow by diffusion in pore water in reducing environments, such as the bottom sediments in limnic areas. Moreover, the factors necessary for the formation of vivianite, *i.e.*, the presence of ferric oxy-hydroxides (Manning *et al.* 1991) and of organic (wood) remains (Nriagu & Dell 1974), and, implicitly the electric field due to organic decomposition (Zelibor *et al.* 1988), all occurred in the sedimentary basin at Capeni. Deposition and diagenesis occurred under fairly oxidizing conditions, since sulfides such as pyrite or marcasite are low in abundance in the vivianite-bearing sequences. However, as Manning *et al.* (1991) pointed out, in some other limnic areas the bottom sediments are sulfide-bearing. Therefore, if sulfur had been available, iron sulfides would have been able to form. Their scarcity, as well as that of the derivative sulfates (*e.g.*, szomolnokite, melanterite, jarosite), may indicate an absence of sulfur in water during deposition. Consequently, at Capeni, iron coming from a vent system precipitated as ferric oxy-hydroxides and then reduced to vivianite, in an environment that was sufficiently oxidizing, to form $(PO_4)^{3-}$. This is entirely consistent with the affirmation of Berner (1981) that vivianite generally occurs in anoxic low-sulfide sediments.

Some supplementary conclusions may be drawn on the basis of the trace-element geochemistry of the vivianite. The enrichment in Ba and the presence of Sr, despite the low Ca content, are not uncommon, since Ba becomes strongly concentrated in some lacustrine sediments such as shale, particularly in black shale. This behavior, which suggests a connection of Ba with organic matter (Puchelt 1974), explains its abundance in the samples of vivianite analyzed. On the other hand, it seems that the concentration of the *REE* is independent of Ca concentration. The deficiency in *REE* may be explained by the low pH, which favors dissolution of carbonates and mobilization of lanthanides. The low pH, which explains the low abundance of the *REE* in shales and sandstones from coal-bearing deposits (Balashov *et al.* 1964), is common during crystallization of vivianite. The marked relative enrichment in heavy *REE* is anomalous only in appearance. According to Balashov *et al.* (1964), an increased acidity, *i.e.*, a higher content of HCO_3^- in natural waters, causes a higher solubility of the heavier lanthanides, relative to the lighter ones. A preferential inflow of the heavy *REE* to the sedimentary basin is then to be presumed. This "excess" would precipitate with the iron and must be incorporated into the vivianite after the reduction of the initial ferric oxy-hydroxides.

All the physical and chemical data presented above show that the analyzed vivianite is partly oxidized. This oxidation probably occurred on exposure of the samples to air after their collection. One can infer that most of the museum and laboratory specimens that were analyzed by various authors were submitted to different degrees of oxidation upon removal from their initial environment.

ACKNOWLEDGEMENTS

This work was supported by the European Community through a fellowship granted to S.M. at Université Catholique in Louvain. S.M. also acknowledges receipt of a grant from the French Government, to facilitate the documentation. Our thanks are due to the staff of Department of Geochemistry, École Nationale de Mines in Saint-Étienne for assistance and for helpful suggestions. The authors gratefully thank Mr. Jacques Wautier (Université Catholique, Louvain) for his assistance with the electron microprobe, Mrs. Gabriela Stelea (Geological Institute, Bucharest) for infrared analyses, Mr. Traian Draghiciu (Geological Institute, Bucharest) for thermal records, Mr. Jacques Moutte (École Nationale de Mines, Saint-Étienne) for ICP data, and Mrs. Erna Calinescu (PROSPECTIUNI SA. Bucharest) for wet-chemical analyses. Last but not least, we are sincerely grateful to Professor Robert F. Martin and to two anonymous reviewers for critical reading and correction of the manuscript.

REFERENCES

APPLEMAN, D.E. & EVANS, H.T., JR. (1973): Indexing and least-squares refinement of powder diffraction data. *U.S. Geol. Surv., Comput. Contrib.* **20** (*NTIS Doc.* **PB-216**).

AUTEFAGE, F. & FONTAN, F. (1985): Comportement de minéraux hydratés au cours de leur analyse à la microsonde électronique. *Bull. Minéral.* **108**, 293-304.

BALASHOV, YU.A., RONOV, A.B., MIGDISOV, A.A. & TURANSKAYA, N.V. (1964): The effect of climate and facies environment on the fractionation of the rare elements during sedimentation. *Geokhimiya* **8**, 951-969 (in Russ.).

BARTH, T.F.W. (1937): Crystallographic studies in the vivianite group. *Am. Mineral.* **22**, 325-341.

BENOIT, P.H. (1987): Adaptation to microcomputer of the Appleman–Evans program for indexing and least-squares refinement of powder-diffraction data for unit-cell dimensions. *Am. Mineral.* **72**, 1018-1019.

BERNER, R.A. (1981): A new geochemical classification of sedimentary environments. *J. Sed. Petrol.* **51**, 359-365.

BOCCHI, G., BONDI, M., FORESTI, E. & NANNETTI, M.C. (1971): Carracteristiche chimiche, termiche, ottiche e roentgenografiche della vivianite di Anloua (Cameroun). *Mineral. Petrogr. Acta* **17**, 109-133.

BORCOS, M., KRÄUTNER, H.G., UDUBASA, G., SANDULESCU, M., NASTASEANU, S. & BITOIANU, C. (1984): Map of the mineral resources. Explanatory note. *In* Geological Atlas of Romania (1:1 000 000). Institute of Geology and Geophysics, Bucharest, Romania.

BRUNEL, R. & VIERNE, R. (1970): Spectres de réflexion infrarouge de minéraux monocristallins ou en poudre (II). *Bull. Soc. fr. Minéral. Cristallogr.* **93**, 328-340.

CADERE, D.M. (1928): Fapte pentru a servi la descrierea mineralogica a României. *Mem. Sect. St. Acad. Rom., ser.* **III, 6.**

DE GRAVE, E., VOCHTEN, R., DESSEIN, H. & CHAMBAERE, D. (1980): Analysis of some oxidized vivianites. *J. Phys.* **C 1**, *Suppl.*, **41**, 407-408.

DONNAY, J.D.H., DONNAY, G., COX, E.G., KENNARD, O. & KING, V.M. (1963): *Crystal Data. Determinative Tables* (2nd ed.). Williams & Heintz, Washington, D.C.

DORMANN, J.L., GASPÉRIN, M. & POULLEN, J.-F. (1982): Étude structurale de la séquence d'oxydation de la vivianite, $Fe_3(PO_4)_2{\cdot}8H_2O$. *Bull. Minéral.* **105**, 147-160.

_______ & POULLEN, J.-F. (1980): Étude par spectroscopie Mössbauer de vivianites oxydées naturelles. *Bull. Minéral.* **103**, 633-639.

FRAZIER, A.W., LEHR, J.R. & SMITH, J.P. (1963): The magnesium phosphates hannayite, schertelite and bobierrite. *Am. Mineral.* **48**, 635-641.

FEJDI, P., POULLEN, J.-F. & GASPÉRIN, M. (1980): Affinement de la structure de la vivianite $Fe_3(PO_4)_2{\cdot}8H_2O$. *Bull. Minéral.* **103**, 135-138.

GAMIDOV, R.S. & MAMEDOV, K.S. (1960): On the structure of vivianite and its derivatives. *Azerbaidzhan Khim. Zh.* **4**, 121-125 (in Russ.).

GONSER, U. & GRANT, R.W. (1967): Determination of spin directions and electric field gradient axes in vivianite by polarized recoil-free γ-rays. *Phys. Stat. Solidi* **21**, 331-342.

HERRMANN, A.G. (1978): Yttrium and lanthanides. *In* Handbook of Geochemistry **II-5** (K.H. Wedepohl, ed.). Springer Verlag, Berlin, Germany (39, 57-71-B-M, O).

HUME, D.N. & KOLTHOFF, I.M. (1957): The use of cacotheline as an oxidation–reduction indicator before the volumetric determination of iron. *Anal. Chim. Acta* **16**, 415-418.

KLEBER, W., WILDE, W. & FRENZEL, M. (1965): Thermal decomposition and oxidation of ferrous iron in vivianite. *Chem. Erde* **24**, 77-93.

MANDARINO, J.A. (1976): The Gladstone–Dale relationship. I. Derivation of new constants. *Can. Mineral.* **14**, 498-502.

________ (1981): The Gladstone–Dale relationship. IV. The compatibility concept and its application. *Can. Mineral.* **19**, 441-450.

Manly, R.L., Jr. (1950): The differential thermal analysis of certain phosphates. *Am. Mineral.* **35**, 108-115.

Manning, P.G., Murphy, T.P. & Prepas, E.E. (1991): Intensive formation of vivianite in the bottom sediments of mesotrophic Narrow Lake, Alberta. *Can. Mineral.* **29**, 77-85.

Mattievich, E. & Danon, J. (1977): Hydrothermal synthesis and Mössbauer studies of ferrous phosphates of the homologous series $Fe^{2+}_3(PO_4)_2(H_2O)_n$. *J. Inorg. Nucl.Chem.* **39**, 569-580.

Maxwell, J.A. (1968): *Rock and Mineral Analysis.* Interscience Publishers, London, U.K.

McCammon, C.A. & Burns, R.G. (1980): The oxidation mechanism of vivianite as studied by Mössbauer spectroscopy. *Am. Mineral.* **65**, 361-366.

Mori, H. & Ito, T. (1950): The crystal structure of vivianite and symplesite. *Acta Crystallogr.* **3**, 1-6.

Nakano, S. (1992): Manganoan vivianite in the bottom sediments of Lake Biwa, Japan. *Mineral. J. (Japan)* **16**, 96-107.

Nembrini, G.P., Capobianco, J.A., Viel, M. & Williams, A.F. (1983): A Mössbauer and chemical study of the formation of vivianite in sediments from Lago Maggiore (Italy). *Geochim. Cosmochim. Acta* **47**, 1459-1464.

Nriagu, J.O. & Dell, C.I. (1974): Diagenetic formation of iron phosphates in recent lake sediments. *Am. Mineral.* **59**, 934-946.

Palache, C., Berman, H. & Frondel, C. (1951): *The System of Mineralogy* **III**. John Wiley & Sons, New York, N.Y.

Piriou, B. & Poullen, J.-F. (1987): Étude infrarouge des modes vibrationnels de l'eau dans la vivianite. *Bull. Minéral.* **110**, 697-710.

Puchelt, H. (1974): Barium. *In* Handbook of Geochemistry **II-4** (K.H. Wedepohl ed.). Springer Verlag, Berlin, Germany (56-B-O).

Radulescu, D. & Dimitrescu, R. (1966): *Mineralogia topografica a Romăniei.* Academic Ed., Bucharest, Romania.

Rao, A.B. (1965): Note on the DTA study of some rare Brazilian phosphate minerals. *Mineral. Mag.* **35**, 427-428.

Ritz, C., Essene, E.J. & Peacor, D.R. (1974): Metavivianite, $Fe_3(PO_4)_2 \cdot 8H_2O$, a new mineral. *Am. Mineral.* **59**, 896-899.

Rodgers, K.A. (1989): The thermochemical behaviour of vivianite and vivianite/metavivianite admixtures from Borne (Netherlands) and Mangualde (Portugal). *Geol. Minjbouw* **68**, 257-262.

________ & Henderson, G.S. (1986): The thermochemistry of some iron phosphate minerals: vivianite, metavivianite, baricite, ludlamite and vivianite/metavivianite admixtures. *Thermochim. Acta* **104**, 1-12.

Rosenqvist, I.T. (1970): Formation of vivianite in Holocene clay sediments. *Lithos* **3**, 327-334.

Sameshima, T., Henderson, G.S., Black, P.M. & Rodgers, K.A. (1985): X-ray diffraction studies of vivianite, metavivianite and baricite. *Mineral. Mag.* **49**, 81-85.

Tien, Pei-Lin & Waugh, T.C. (1969): Thermal and X-ray studies on earthy vivianite in Graneros Shale (Upper Cretaceous), Kansas. *Am. Mineral.* **54**, 1355-1362.

________, ________ & Dilts, R.L. (1969): Vivianite in Graneros Shale (Upper Cretaceous), central Kansas. *Kansas Geol. Surv. Bull.* **194**, 21-24.

Vochten, R., De Grave, E. & Stoops, G. (1979): Petrographic, chemical and Mössbauer study of some oxidized vivianite nodules from Retie (Province of Antwerp, Belgium). *Neues Jahrb. Mineral., Abh.* **137**, 208-222.

Yamaguti, T. (1936): *Proc. Phys.-Math. Soc. Japan* (3), **18**, 372-379.

Zelibor, J.L., Senftle, F.E. & Reinhardt, J.L. (1988): A proposed mechanism for the formation of spherical vivianite crystal aggregates in sediments. *Sediment. Geol.* **59**, 125-142.

Received March 7, 1996, revised manuscript accepted January 25, 1997.